


RESEARCH ARTICLE

Comparing camera-based ungulate density estimates: a case study using island populations of bighorn sheep and mule deer

Jessica Coltrane¹  | Nicholas J. DeCesare² | Jon S. Horne³ | Paul M. Lukacs⁴

¹Montana Fish, Wildlife and Parks, Kalispell, MT 59901, USA

²Montana Fish, Wildlife and Parks, Missoula, MT 59804, USA

³Idaho Department of Fish and Game, Lewiston, ID 83501, USA

⁴Wildlife Biology Program, W. A. Franke College of Forestry and Conservation, University of Montana, Missoula, MT 59812, USA

Correspondence

Jessica Coltrane, Montana Fish, Wildlife and Parks, 490 N. Meridian, Kalispell, MT 59901, USA.

Email: jcoltrane@mt.gov

Funding information

Montana Fish, Wildlife and Parks

Abstract

Camera-based abundance estimators are an alternative methodology of growing interest in both research and management applications. The statistical formulations of camera-based abundance estimators using time-lapse data should theoretically produce precise and unbiased estimates; however, production of unbiased results also requires meeting several important assumptions, and real-world case studies evaluating such results remain relatively few. We applied instantaneous sampling (IS) and space-to-event (STE) estimators to remote camera data collected in April 2021 via time-lapse sampling of closed populations of bighorn sheep (*Ovis canadensis*) and mule deer (*Odocoileus hemionus*) on Wild Horse Island in western Montana, USA, and compared results for bighorn sheep to aerial and ground-based counts. Point estimates from camera-based approaches underestimated bighorn sheep populations by 32–44% (IS estimator) and 62–69% (STE estimator) relative to aerial and ground counts. Patchy spatial distribution and group-living behavior of sheep resulted in a high degree of noise surrounding the IS estimate. In comparison, a low point estimate with relatively narrow confidence intervals suggested potential sensitivity of the STE estimator to violating assumptions of independence among individual animals and sampling occasions. Estimates of mule deer had improved precision over sheep estimates, as indicated by lower estimated coefficients of variation of the mean (CV_{mean}) derived from the analytic SE estimator. Using 15-m viewsheds and the IS estimators, mule

deer density estimates came with a 26% CV_{mean} compared to 43% CV_{mean} for bighorn sheep. This discrepancy may be a result of differences in distribution, behavior, and relative abundance between the 2 species. Accounting for group size and increasing time between sampling may improve accuracy of density estimates and adhere better to model assumptions when estimating precision. In addition, factors influencing viewshed and resulting density extrapolations must be considered carefully. While camera-based methods theoretically provide an alternative way to estimate density when traditional methods are impractical, our results suggest that more work is needed to ensure density estimates are accurate and precise enough to inform population management.

KEYWORDS

abundance, camera trap, *Ovis canadensis*, space-to-event, time-lapse, unmarked, viewshed area

Estimates of population abundance are a foundational component of many wildlife monitoring and management programs (Pollock et al. 2002). For ungulate species, count data are commonly collected by wildlife managers via aerial or ground surveys to monitor population abundance and trends (DeCesare et al. 2016, Zabransky et al. 2016, Forsyth et al. 2022). Camera-based abundance estimators are an alternative methodology of growing interest in both research and management applications, particularly in environments where other survey methods are hampered by poor visibility of animals or other logistical constraints (Gilbert et al. 2020).

Remote cameras are a powerful means to detect and count species across diverse landscapes and habitats, yet the data collected from cameras present challenges when seeking unbiased population estimates (Sollman et al. 2013). Such challenges include the inability to identify individual animals amongst detections for many species and uncertainty in how the detection process is affected by heterogeneity in both animal movement and camera motion-trigger functionality (Burton et al. 2015). A variety of new statistical techniques have been developed to estimate density of unmarked animals using remote cameras, including techniques that specifically address imperfect capture probabilities ubiquitous in motion-triggered photography (Hofmeester et al. 2017, 2019, Howe et al. 2017, Nakashima et al. 2018). An alternate approach that addresses heterogeneity in capture probability is to collect time-lapse pictures (e.g., taken every 5 minutes), which are sampled and recorded without motion triggers. The instantaneous sampling (IS) and space-to-event (STE) estimators were developed to evaluate time-lapse sampled data (Moeller et al. 2018) and have been applied across a diversity of study systems (Amburgey et al. 2021, Ausband et al. 2022, Leo et al. 2022). This approach removes components of camera-based sampling that lead to high heterogeneity in capture probability (i.e., variation in the effectiveness of motion-triggered photography) and overall reduction of conditions under which capture probability is <1 (Moeller et al. 2023).

The statistical formulations of camera-based abundance estimators using time-lapse data should theoretically produce precise and unbiased estimates. However, production of unbiased results also requires meeting several important assumptions, and real-world case studies evaluating such results remain relatively few. Moeller et al. (2018) presented a case study wherein camera-based IS and STE estimates both underestimated sightability-corrected counts of elk (*Cervus canadensis*), yet they admittedly violated assumptions of random camera placement

(IS and STE), perfect capture probability (IS and STE), and independent movement among individuals (STE only) with unmeasured effects (Lyet et al. 2024). Leo (2022) found IS and STE camera-based point estimates of feral sheep (*Ovis aries*) abundance to be slightly higher and lower, respectively, to a population estimate produced from aerial distance sampling; however, confidence intervals of all estimates overlapped. Grouping behavior of sheep in this study may have violated the assumption of independent movement for STE estimates and only daytime pictures were analyzed, both of which may have affected results. Amburgey et al. (2021) found both IS and STE estimators to be biased high when estimating brown tree snake (*Boiga irregularis*) abundance; however, they violated the assumption that animals moved randomly with respect to camera sites by using lures to increase detections. Remaining studies to date focus predominately on motion-triggered camera data, which may be necessary to generate sufficient images of rare species but come with heavy baggage of heterogeneity in capture probability and corresponding sampling uncertainties (Moeller et al. 2023).

We applied IS and STE estimators to remote camera data collected via time-lapse sampling of closed populations of bighorn sheep (*Ovis canadensis*) and mule deer (*Odocoileus hemionus*) occupying Wild Horse Island in western Montana, USA. Island ungulate populations present favorable opportunities to apply such methodologies to truly closed populations. For bighorn sheep, the resulting estimates could also be readily compared to minimum count data from other commonly applied approaches, including aerial and ground surveys. Our first objective was to produce counts or statistical estimates of abundance for bighorn sheep on Wild Horse Island, Montana, using 3 methods including traditional aerial survey-based minimum counts, ground survey-based minimum counts, and time-lapse remote camera-based population estimates. Our second objective was to assess the agreement and coverage of traditional survey methods with camera-based estimates using multiple estimators (IS, STE). Our third objective was to assess how logistical considerations of day versus night, viewshed maximum radius, and overdispersion or patchiness in detections affected camera-based estimates for bighorn sheep and mule deer.

STUDY AREA

Wild Horse Island was an 8.7-km² state park located within Flathead Lake and within the exterior boundary of the Flathead Indian Reservation in northwest Montana (Figure 1). Fifty-six small, 0.004-km², private parcels exist along the island's shoreline but did not penetrate the interior of the island. The southern and predominately south-facing portion of the island consisted of grassland vegetation over mixed topography, interspersed with ponderosa pine (*Pinus ponderosa*) and Douglas-fir (*Pseudotsuga menziesii*). This was juxtaposed with the northern and predominately north-facing portion of the island, which was heavily timbered with the same conifer species. The shoreline of the island was 885 m above sea level, and there were 6 summits ranging from heights of 999 m to 1,141 m. Average yearly precipitation on the island was 400 mm, and average daily temperatures ranged from -4°C to 19°C. The island was home to bighorn sheep, mule deer, coyotes (*Canis latrans*), red foxes (*Vulpes vulpes*), and the occasional mountain lion (*Puma concolor*), and black bear (*Ursus americanus*).

Bighorn sheep were successfully introduced to Wild Horse Island in 1939 by a private landowner. These sheep are isolated to the island, which is ≥ 2 km from the nearest mainland shoreline. In 1977, the island became a state park, and since that time annual helicopter surveys have been conducted to monitor the sheep population. These surveys are typically completed during the winter or spring green-up period (early to mid-April) and sightability is considered good because most of the sheep are found on the southern half of the island where forest cover is sparse. Bighorn sheep management on the island includes a population target of 110 individuals, and management activities occasionally include removal of sheep from the island for population augmentation or reintroduction at sites elsewhere (Montana Fish, Wildlife and Parks 2010). Since 2015, multiple mountain lions have been observed on the island and have been implicated in a precipitous decline in sheep numbers and overall recruitment. All data for this study were collected during April 2021.

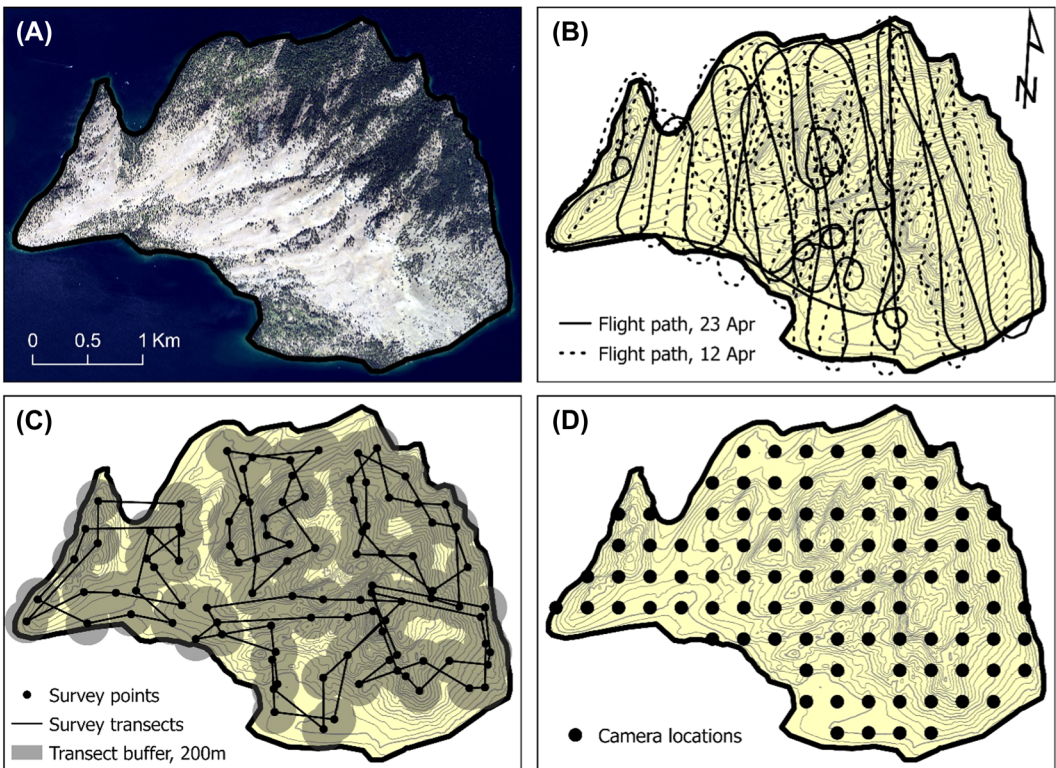


FIGURE 1 Wild Horse Island study area showing A) aerial imagery, B) aerial survey flight paths, C) ground survey transects and point locations, and D) remote camera locations in Montana, USA, 2021.

METHODS

Aerial and ground surveys

We conducted transect-based aerial surveys of bighorn sheep in a Hughes 500 helicopter in April 2021, coinciding with ongoing camera sampling. Survey replicates were conducted on 12 April and 23 April by a crew including a primary observer and a pilot, functioning as a second observer. We flew north-south transects with the intention of complete visual coverage of the entirety of the island. Transect widths were 350 m in open grasslands and 250 m in forested areas. Because of the tendency of bighorn sheep to flee from the helicopter when in open terrain, we used wider transects in open areas to take advantage of increased sightability and minimize disturbance to animals. We recorded the flight path and sheep locations using hand-held global positioning system (GPS) units and classified sheep as adult males, adult females, and yearlings (i.e., 11 months old). Because of the difficulty of distinguishing between young males and females from the air, it is possible that young males that had not yet dispersed from female bands were classified as females. We considered numbers of sheep observed during each flight as a minimum count. We then pooled data across flights by taking the higher count per flight of each classification of adult males, adult females, and yearlings to produce an across-flights minimum count that leveraged the highest count of each age- and sex-specific grouping.

We conducted ground surveys for bighorn sheep on 20 April 2021 with 12 independent observers split into 6 2-person teams. We created survey routes for each observer by first dividing the island evenly into a grid of 100 equal-area cells (284×284 m) and randomly selecting 52 spatially distributed grid cells for targeted surveys.

We then assigned each team to sample 10-12 cells and selected 2 survey points (one per observer) to maximize site distance and viewshed within each cell. Observers walked independently along pre-determined survey routes and recorded counts of all observed bighorn sheep, including those along routes, within cells and at survey points. Along routes we recorded groups within 200-m transect widths on each side of the survey route (Figure 1). All observers were in contact with adjacent teams to avoid double counting of sheep. Observers documented each group of sheep observed, group composition, and time of observation. When teams observed a group of sheep, they recorded the location of observer and bearing and distance to sheep so that the location of each sheep group could be determined *post hoc*. Sheep on the island are highly habituated to human hikers and typically did not flee from people approaching closely.

Camera surveys

We used a systematic sampling design to evenly distribute camera-based density sampling across the entire island study area. We used the same grid of 100 equal-area cells (284×284 m) as described for ground surveys but sampled every cell with a camera location at the cell centroid. We removed 3 of these centroid locations from the sample because of field logistics (e.g., private land and high probability of camera theft) and deployed cameras on the remaining 97 locations. We disabled the motion sensors of each camera and programmed cameras to collect time-lapse images every 5 minutes during a 1-month study period of 1 April–30 April 2021. We considered each picture captured at this 5-minute interval as a sampling occasion, and pictures capturing animals as detections.

When deploying cameras in the field, we established cone-shaped viewsheds at each location with a maximum radius of 30 m from the camera location. We placed markers (reflective snow-stakes and tape) at fixed distances of 15 m, 20 m, and 30 m from the camera to delineate 3 viewsheds of different radii that could be identified within images (Figure 2). We then measured the viewshed area by dividing the camera's field of view into 6 cone-shaped sectors and measuring distances of different obstructions that reduced viewable area, as described by Moeller et al. (2023). We used these data to measure 3 definitions of viewshed area, according to the maximum radii of 15 m, 20 m, and 30 m and accounting for obstructions due to vegetation and topography at each distance.

We manually classified species detections in all images, with output data for each image including counts of all bighorn sheep and mule deer within each of the 3 field-measured viewsheds of maximum radii 15 m, 20 m, and

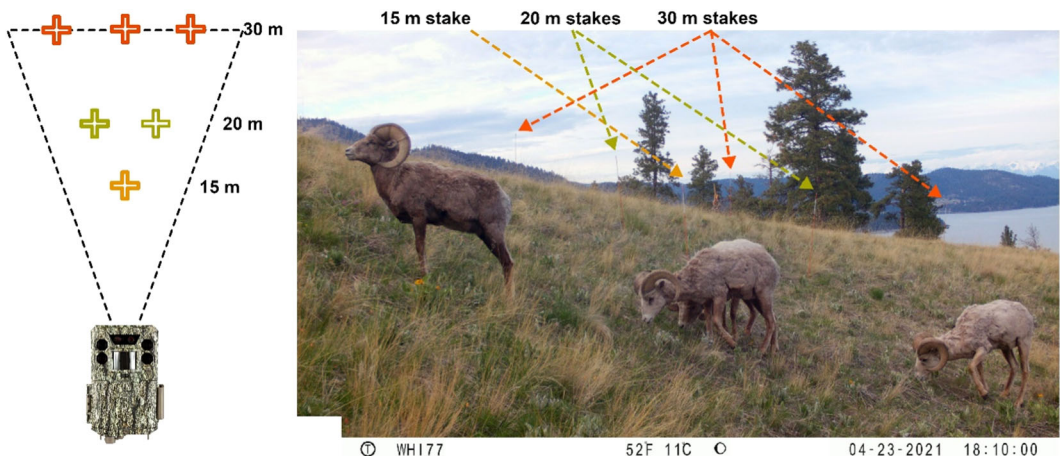


FIGURE 2 Schematic of camera plots on Wild Horse Island, Montana, USA, in 2021 showing placement of reflective snow stakes to mark multiple viewshed radii at distances of 15 m, 20 m, and 30 m from the camera.

30 m, which equaled areas of 77.5 m², 137.7 m², and 309.9 m², respectively. We also recorded periods of camera misalignment (e.g., bumped out of alignment by wildlife) or obscured field of view (e.g., lens covered by snow) that were later censored from analyses. When classifying images, we determined that the shortest viewshed radius of 15 m could not be completely illuminated by nighttime flashes for a subset of cameras ($n = 15$), and we censored all night images from these sites. In most cases this was caused either by a camera aimed too low or by a branch or tree in the immediate foreground that caused areas farther away to be underexposed in images. We extrapolated density estimates to abundance by multiplying density by the 3-dimensional surface area of Wild Horse Island (9.359 km²), which we estimated using the 3D Analyst extension for ArcGIS 10.8.2 (Esri, Redlands, CA, USA) and a digital elevation model of 3-m resolution.

Statistical analyses

We estimated density for bighorn sheep and mule deer using viewsheds of 15 m, 20 m, and 30 m and using both the IS and STE estimators. The IS estimator treats density as the mean of observed densities (i.e., total animals counted within the viewshed divided by the respective viewshed area) across each camera i and sampling occasion j according to Moeller et al. (2018). We estimated analytic standard errors for the IS estimator using $i = 1, 2, \dots, M$ cameras as:

$$\text{Var}(\hat{D}) = \frac{M}{L^2(M-1)} \sum_{i=1}^M (J \cdot a_i)^2 \left(\frac{n_i}{J \cdot a_i} - \frac{N}{L} \right)^2, \quad (1)$$

where \hat{D} is density, $J \cdot a_i$ is the summed area of camera i across all occasions, L is the sum of all $J \cdot a_i$ area totals across cameras, count n_i is the count of animals over all occasions at camera i , and N is the total count of animals over all animals and occasions (Moeller et al. 2018). We estimated density across the entire study period and for each day of the study. To account for temporal autocorrelation of 5-minute time lapse sampling occasions, we also estimated standard errors using bootstrapping to resample data across cameras. We resampled cameras with replacement, generated 5,000 bootstrapped estimates of density, and used resampled data to estimate the bootstrapped standard error for each density estimate. We then estimated 95% confidence intervals surrounding point estimates of density (\hat{D}) assuming log-normal distribution of estimates (Buckland et al. 1993).

$$\text{CI}_{\text{Lower}} = \frac{\hat{D}}{\exp\left(1.96 \times \sqrt{\ln\left[1 + \left(\frac{SE}{\hat{D}}\right)^2\right]}\right)} \quad (2)$$

and

$$\text{CI}_{\text{Upper}} = \hat{D} \times \exp\left(1.96 \times \sqrt{\ln\left[1 + \left(\frac{SE}{\hat{D}}\right)^2\right]}\right). \quad (3)$$

The STE estimator is an adaptation of time-to-event, or survival, models founded upon the repeated summation of space sampled by randomly sorted camera viewsheds until a detection of the target species occurs within each sampling occasion (Moeller et al. 2018). The STE estimator assumes a Poisson distribution of animal detections and that the space between detections is an exponentially distributed function of the mean number of animals (Moeller et al. 2018). We estimated STE-based density and analytical standard errors using the spaceNtime package (Moeller and Lukacs 2021) for program R 4.2.1 (R Core Team 2022). We similarly used Equations 2 and 3 to estimate log-normal confidence intervals for STE estimates. We defined sampling effort (i.e., time intervals during which cameras

were active) for each camera, excluding occasions when cameras were misaligned or intermittently obstructed. We estimated the coefficient of variation of the mean ($CV_{\text{mean}} = SE/\text{mean}$; Twining et al. 2022) for density estimates of bighorn sheep and mule deer using 15-m viewsheds and mean and SE estimates from the IS estimator and analytic standard error estimates (Equation 1).

RESULTS

We conducted aerial surveys under good survey conditions and maintained similar flight paths between surveys (Figure 1). Daily temperatures in April 2021 ranged from -7°C to 24°C , and we did not observe any significant weather events that may have affected sheep distribution during the study period. During the first survey, we observed 63 sheep (26 males and 37 females), compared to 66 sheep (19 males, 45 females, and 3 yearlings) during the second survey. Combined, these surveys produced a minimum count of 74 sheep, including 26 males, 45 females, and 3 yearlings.

Six, 2-observer teams conducted a ground survey for bighorn sheep on 20 April 2021. After accounting for sheep observed by multiple observers, teams observed 77 sheep (22 adult males, 45 adult females, and 10 yearlings; Figure 3). Group size ranged from 5 to 18 sheep, with an average group size of 11 sheep.

We recovered camera-based density data from 93 of 97 deployed cameras. After filtering data to remove sampling occasions with poor visibility or misaligned viewsheds, these data included 668,523 images across 8,639 5-minute sampling sessions during the 30-day study period. Point estimates of density for bighorn sheep and mule deer using the IS estimator with 15-m viewsheds were $4.59/\text{km}^2$ and $19.9/\text{km}^2$, respectively, which translated to abundance estimates of 43 bighorn sheep and 186 mule deer (Table 1). Standard error estimates were similar between the analytical estimator for IS and bootstrapped resampling for both bighorn sheep ($SE_{\text{analytical}} = 1.97$, $SE_{\text{bootstrap}} = 1.93$) and mule deer ($SE_{\text{analytical}} = 5.19$, $SE_{\text{bootstrap}} = 5.15$). Using 15-m viewsheds and the IS estimators, mule deer density estimates came with a 26% CV_{mean} compared to 43% CV_{mean} for bighorn sheep. The point estimate of bighorn sheep density using the STE estimator ($D_{\text{STE}} = 2.60$) was considerably lower than that for IS, as was the standard error ($SE_{\text{STE}} = 0.23$). We observed similar results for mule deer, where STE-based point estimates ($D_{\text{STE}} = 12.8$) and standard error ($SE_{\text{STE}} = 0.51$) were both considerably less than that for IS ($D_{\text{IS}} = 19.9$, $SE_{\text{IS}} = 5.2$; Table 1; Figure 3).

Comparison of aerial survey, ground survey, and camera-based estimates of bighorn sheep showed mixed results (Figure 3). Aerial and ground count data yielded minimum counts without estimable metrics of uncertainty. Despite those limitations, minimum counts from 2 pooled aerial surveys ($N = 74$) and a single ground survey ($N = 77$) were quite similar. Point estimates of abundance from cameras using 15-m viewsheds were lower than minimum counts for both the IS ($N_{\text{IS}} = 43$) and STE ($N_{\text{STE}} = 24$) estimators (Figure 3). The STE-based standard errors were small and confidence intervals did not include minimum count estimates from aerial and ground-based methods (Figure 3). However, 95% log-normal confidence intervals for IS-based estimates included aerial and ground survey minimum counts under both analytic (95% CI = 19.2–96.3) and bootstrap (95% CI = 19.5–94.7) estimates of variance (Figure 3). Density estimates restricted to sampling sessions at night were higher than those estimated during the day for both bighorn sheep and mule deer (Figure 4). Nighttime density estimates decreased with increasing viewshed area for both bighorn sheep and mule deer, indicating imperfect detection beyond 15 m during periods of darkness (Figure 4). This effect was intuitively less pronounced during daytime, but a consistent decrease in density estimates with increasing viewshed area nonetheless remained (Figure 4).

Bighorn sheep detections were concentrated on similar south-facing, steep, and open vegetation types across aerial survey, ground survey, and remote camera methodologies, whereas mule deer detections via camera were more evenly distributed (Figure 5). Cameras detected a small degree of bighorn sheep presence in forested and north-facing environments distinct from any groups observed during aerial or ground surveys (Figure 5). Variation was high in camera-based estimates of density across the 30-day study period (Figure 6). Estimated density was 0

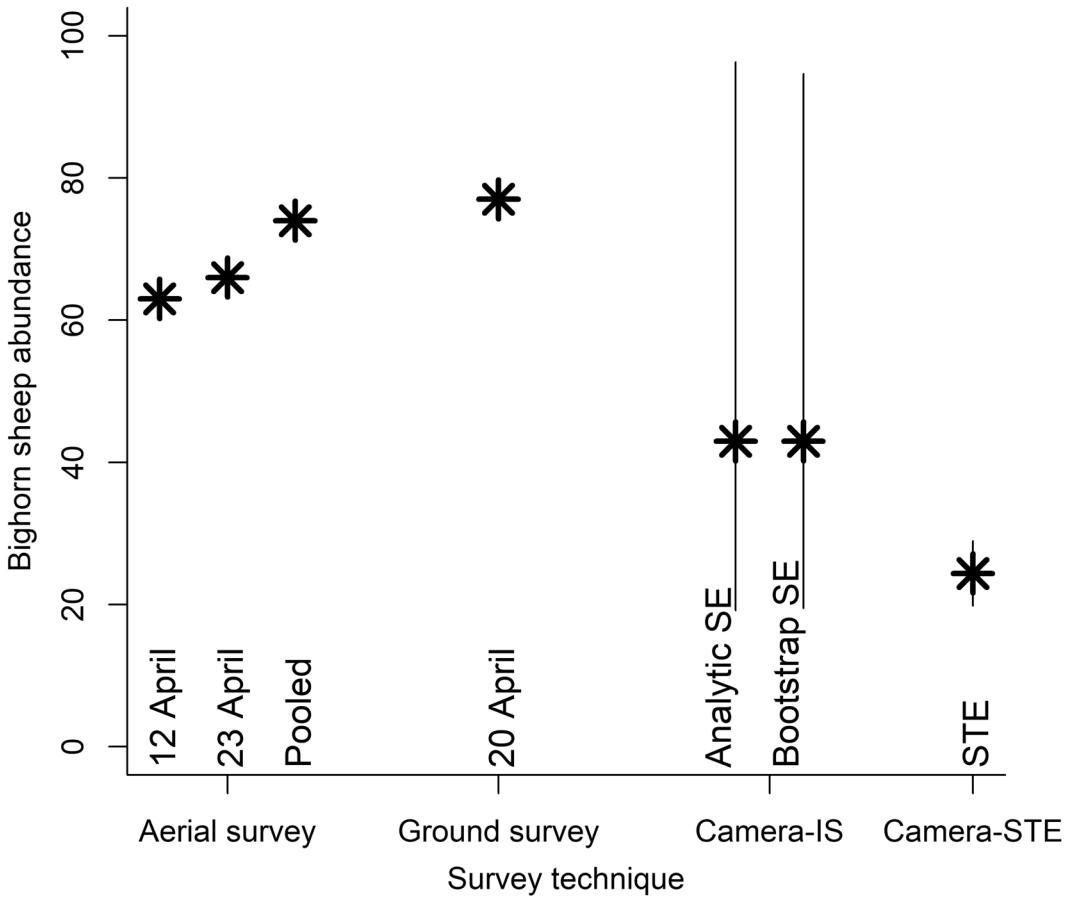


FIGURE 3 Confidence intervals surrounding bighorn sheep population estimates on Wild Horse Island, Montana, USA, in 2021 from the instantaneous estimator for camera-based density estimation (camera-IS; using both analytic and bootstrap approaches to variance estimation) included minimum counts collected via aerial surveys and ground surveys, whereas confidence intervals using the space-to-event (STE) estimator did not.

(i.e., no detections) during 18 of the 30 days, and estimates ranged from 0.5–42.7 sheep/km² during the other 12 days with non-zero density estimates (Figure 6).

DISCUSSION

Point estimates from camera-based approaches underestimated bighorn sheep populations by 32–44% (IS estimator) and 62–69% (STE estimator) relative to aerial and ground counts. However, 95% confidence intervals for bighorn sheep abundance using the IS estimator overlapped aerial- and ground-based minimum counts, while those from STE estimates did not (Figure 3). These results highlight the impact of sampling variation on abundance estimates when using cameras to monitor wildlife populations. In theory, random or systematic sampling of camera locations combined with time-lapse sampling of viewshed images at each location yields unbiased samples of animal density over space and time (Moeller et al. 2018); however, sampling animal density in a small viewshed area inherently produces noise (e.g., Figure 6). Such noise is further amplified in real-world settings as animal counts become clumped, or over-dispersed, owing to biological patterns, such as habitat heterogeneity and social grouping

TABLE 1 Results of camera-based monitoring of bighorn sheep and mule deer according to viewshed maximum radius (r_{max}) and showing the number of images with detections and estimates (and analytical 95% log-normal confidence intervals) of density (D) and abundance (N) of bighorn sheep from the instantaneous sampling estimator (D_{IS} , N_{IS}) and space-to-event estimator (D_{STE} , N_{STE}), Wild Horse Island, Montana, USA, 2021.

| r_{max} | Images | D_{IS} | D_{STE} | N_{IS} | N_{STE} |
|---------------|--------|-------------------|-------------------|------------------|------------------|
| Bighorn sheep | | | | | |
| 15 m | 130 | 4.59 (2.0, 10.3) | 2.60 (2.2, 3.1) | 42.9 (19, 96) | 24.4 (21, 29) |
| 20 m | 149 | 2.95 (1.3, 6.5) | 1.72 (1.5, 2.0) | 27.6 (12, 61) | 16.1 (14, 19) |
| 30 m | 214 | 2.56 (1.3, 5.0) | 1.17 (1.0, 1.3) | 24.0 (12, 47) | 11.0 (10, 12) |
| Mule deer | | | | | |
| 15 m | 646 | 19.9 (12.0, 32.9) | 12.8 (11.8, 13.8) | 185.8 (112, 308) | 119.1 (111, 129) |
| 20 m | 859 | 17.4 (11.3, 26.6) | 9.89 (9.2, 10.6) | 162.5 (106, 249) | 92.6 (86, 99) |
| 30 m | 1,348 | 14.8 (10.6, 20.7) | 7.22 (6.8, 7.6) | 138.9 (99, 194) | 67.5 (64, 71) |

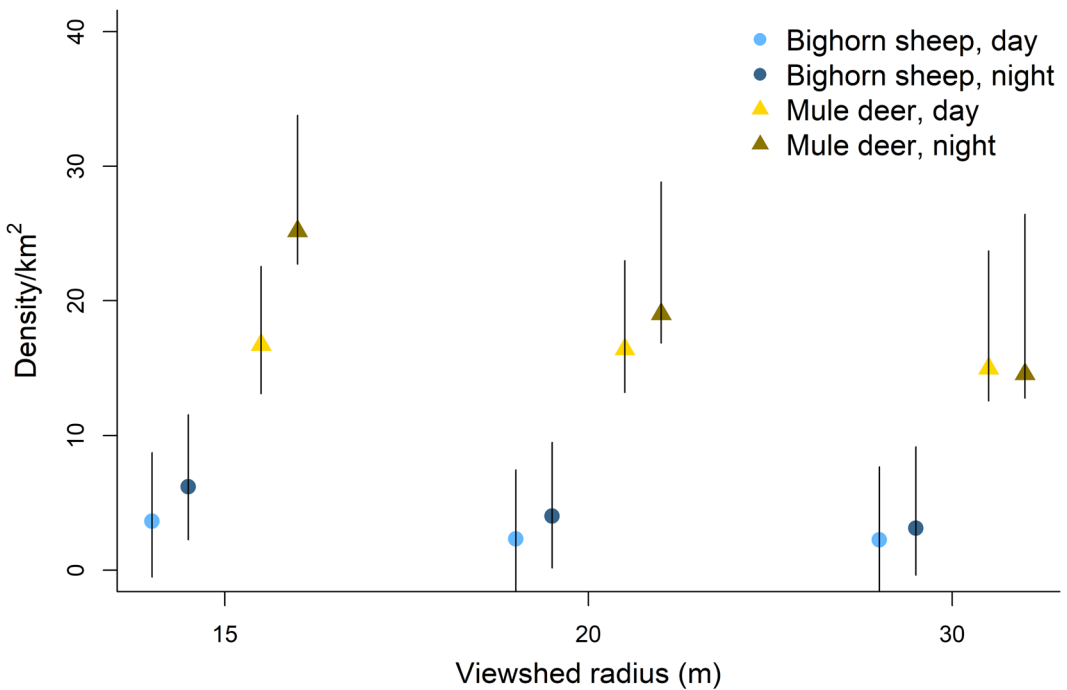


FIGURE 4 Camera-based density estimates for bighorn sheep and mule deer on Wild Horse Island, Montana, USA, in 2021 decreased with increasing maximum viewshed radius (15 m, 20 m, and 30 m), particularly when analyses were restricted to images collected during the night as compared to those collected during the day.

of individuals (Loonam et al. 2021). We found bighorn sheep tended to congregate in groups and select for steep and open landscapes on Wild Horse Island (Figure 5), as has been shown in other areas (DeCesare and Pletscher 2005, 2006, Lula et al. 2020). This contributed to large uncertainty around density estimates ranging from 0–42.7 animals/km² (Figure 6) and created wide IS confidence intervals.

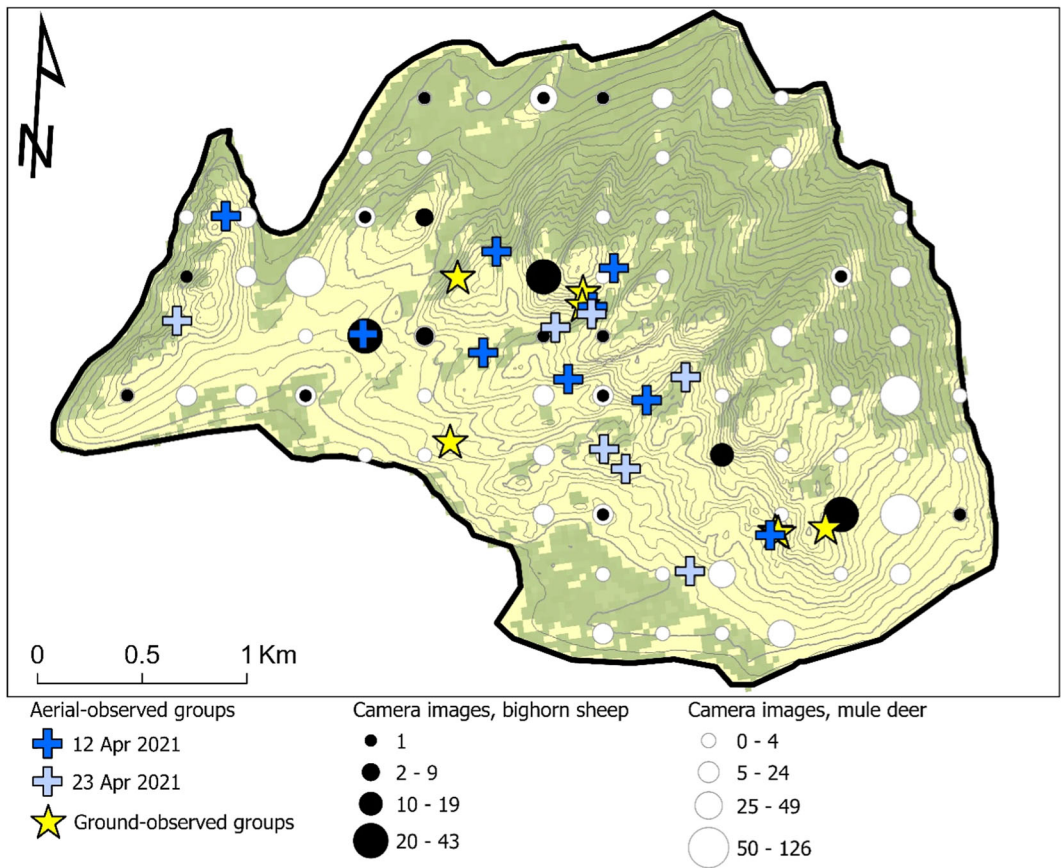


FIGURE 5 Spatial locations of bighorn sheep detected via aerial surveys, ground surveys, and camera-based monitoring on Wild Horse Island, Montana, USA, in 2021 show heterogeneous clustering of bighorn sheep detections in steep and open (yellow) portions of the study area compared to more homogenous distribution of mule deer detections in both open and forested (green) areas.

In comparison, the STE estimator resulted in a low point estimate with relatively narrow confidence intervals that did not overlap counts from aerial and ground surveys. These results suggest potential sensitivity of this estimator to violating assumptions of independence among individual animals and sampling occasions. The STE estimator assumes that animals move independently and does not incorporate information regarding total number of animals in cases when a detection includes more than a single individual in the measured viewshed (Moeller et al. 2018). It has been rigorously shown that bighorn sheep individuals rarely move independently because of their social behavior (DeCesare and Pletscher 2005). This behavior may effectively translate STE-based density estimates to actually be of groups rather than individuals, potentially explaining the relatively low point estimate. Furthermore, the STE estimator assumes independence among sampling sessions, such that animals are redistributed amongst the study area between sessions. In our case, detections (and lack of detections) among 5-minute time-lapse images are surely autocorrelated, exemplified by observations of animals bedded or foraging in front of cameras across sequential images. A similar phenomenon of spatiotemporal autocorrelation was observed in a camera-based study of wolves (*Canis lupus*), where a single camera out of 215 deployed was responsible for >50% of the detections (Ausband et al. 2022). This autocorrelation has the potential to strongly influence point estimates and bias analytical estimates of variance low; this also may partially explain relatively narrow confidence intervals surrounding STE estimates (Figure 3). Increasing the timespan between sampling occasions may help

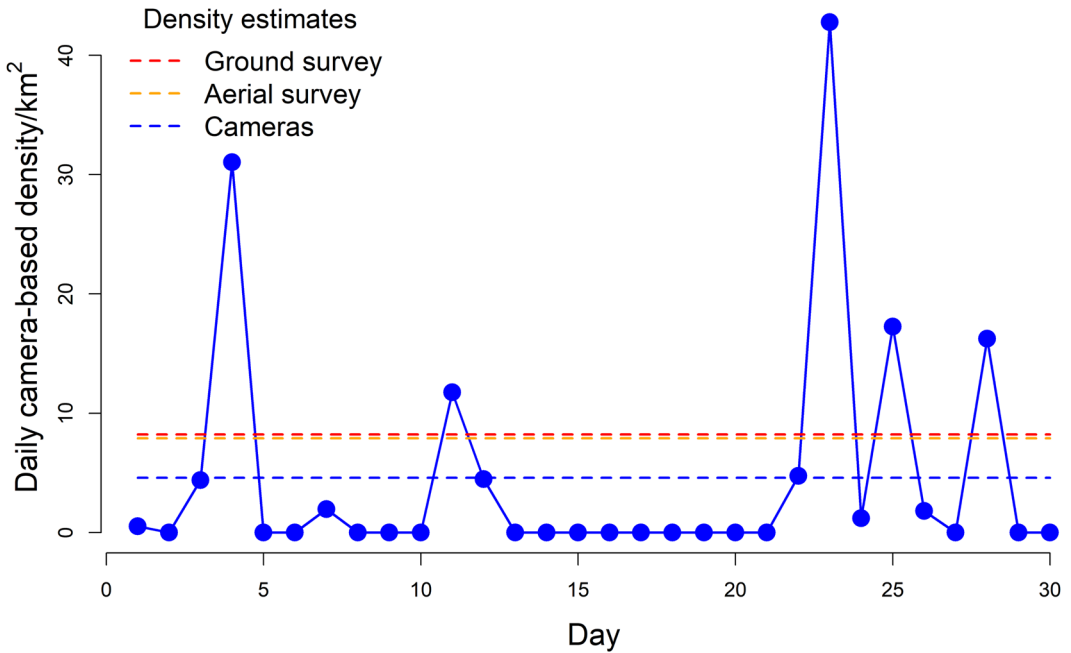


FIGURE 6 Daily density estimates of bighorn sheep on Wild Horse Island, Montana, USA, in 2021 resulting from camera-based monitoring show high levels of temporal sampling variation relative to reference values of density observed during aerial and ground surveys.

alleviate this issue of temporal autocorrelation but may increase the violation of other assumptions, such as population closure. Longer study periods may affect results via changes in population size due to immigration, emigration, births, and deaths. Bootstrapping has been suggested as a means to generate appropriate variance estimates when faced with autocorrelation (Moeller et al. 2018, Ausband et al. 2022); however, resampling cameras with replacement, including identical copies of monitoring histories across resampled data replicates, creates a problem unique to STE analyses where only the first detection is used. An alternate means of correcting STE estimates for autocorrelation across sampling sessions is needed.

The importance of 4 methodological details on camera-based abundance results also became clear during this study. First, we measured viewshed area at each camera site to account for site-specific variation in vegetative or topographic obstructions. In our study this resulted in a 3%, 5%, and 10% proportionate decrease in area sampled for viewsheds of 15-m, 20-m, and 30-m radii, respectively, and a corresponding 3%, 5%, and 10% increase in density estimates. In a similar study in a more heavily forested environment, Moeller et al. (2023) showed 29% proportionate changes in viewshed area and density, driven by greater reduction in viewshed areas from denser vegetation. Second, density estimates decreased as viewshed radii increased, particularly at night, which indicated that the realized viewshed at night was likely less than our maximum 30-m radius (Figure 4). Practitioners of this approach need to consider flash distances carefully and ensure that the full area of viewsheds are truly visible across data streams, particularly when including night sampling. Third, when measuring viewshed areas, we used 3-dimensional distances to mark viewshed boundaries; for example, using a measuring tape to mark a 15-m distance from the camera includes the effect of changes in elevation in that distance. Extrapolating such density estimates to the full study area required a 3-dimensional measure of study area. In our case, the 3-dimensional area of Wild Horse Island (9.36 km²) was 6% greater than 2-dimensional estimates (8.83 km²), which resulted in a 6% proportionate increase in abundance estimates when extrapolating camera-based density estimates to abundance of the entire island. Fourth, in an open environment like the grasslands of this study area, it was often possible to

detect animals beyond the measured viewshed area. Restricting our analysis to animals within viewsheds reduced the counts of animals from 3,664 individual bighorn sheep within all images to 474 sheep within measured viewsheds. This discrepancy highlights the paramount importance of linking animal detections and counts to the viewshed areas that are measured when seeking camera-based density estimates.

Patterns in bighorn sheep estimates were largely upheld by those for mule deer; however, because we did not apply multiple field methods to enumerate mule deer, we have no direct comparisons of abundance. Overall, estimates suggesting mule deer were more abundant than sheep agree with biologist perceptions concerning their relative abundances on the island. Mule deer estimates did come with improved precision, as indicated by a lower estimated coefficient of variation of the mean (CV_{mean}) derived from the analytic SE estimator. Using 15-m viewsheds and the IS estimators, mule deer density estimates came with a 26% CV_{mean} compared to 43% CV_{mean} for bighorn sheep. In this study area, mule deer estimates likely yielded improved precision for multiple reasons: 1) mule deer appeared to use habitat more generally, which resulted in more even spatial distribution of this species across the sampling frame of cameras (Figure 5), 2) the higher overall density of mule deer likely yielded more frequent detections and less overdispersion or variability in patterns of detection by cameras, and 3) the smaller average group size for mule deer (2.68) compared to that for bighorn sheep (4.03), in combination with higher overall abundance, also yielded more groups on the landscape available for detection with higher consistency by cameras. These differences highlight that animal life histories and study area heterogeneity can affect the precision achievable with this technique across systems.

MANAGEMENT IMPLICATIONS

While camera-based methods may be a practical means to estimate abundance, more work is needed to ensure those estimates adequately reflect true density and are both accurate and precise enough to be useful to biologists and applicable to population management. Biologists often use point estimates when managing populations, and therefore accurate estimates or ones with tight confidence intervals are paramount. Without accurate estimates, wildlife managers may employ incorrect harvest or disease management strategies resulting in unwanted population growth or decline. Our results emphasize the importance of understanding how a population's distribution and individuals' behavior affect the efficacy of alternative methods for estimating abundance. Agencies must consider these factors when designing protocols to monitor ungulate populations.

In our study of a small, group-living sheep population, the point estimates generated by the IS and STE models were much smaller than the actual population. This underestimation combined with poor, or potentially biased, precision estimates could lead to mismanagement of this sheep population. For example, bighorn sheep on Wild Horse Island are translocated to repopulate other populations that have been affected by disease events. The statewide management plan recommends removing sheep when the population exceeds 110 individuals. If sheep removals were dependent on our camera-based abundance estimates, sheep could become overabundant, resulting in habitat alteration and lost opportunities to augment struggling populations elsewhere. If the estimate produced by the models overestimates abundance, sheep could be removed from the island, which could reduce the population beyond management objectives. In other areas of Montana, bighorn sheep are managed through selective harvest. Underestimating these populations could lead to overabundance of sheep resulting in lost harvest opportunity, possible habitat effects, and increased disease occurrence, whereas overestimating populations could result in over-harvest and significant population declines.

ACKNOWLEDGMENTS

We would like to thank M. R. Ebinger, E. S. Lula, T. Chilton-Radant, W. Cole, N. J. Anderson, C. D. Neu, N. P. Munh, F. M. Inglefinger, D. Messmer, C. Crane, B. Sterling, S. Johnson, C. Peterson, A. R. Sullivan, and S. Staven for field

assistance. S. Thompson provided useful discussion and feedback concerning this research. This project was funded by Montana Fish, Wildlife and Parks.

CONFLICT OF INTEREST STATEMENT

The authors declare no conflicts of interest.

ETHICS STATEMENT

Our data collection was non-invasive, solely observational, and did not use lures or attractants of any kind. We did not disturb or negatively affect individual animals or populations, and we followed the American Society of Mammalogists' guidelines for conducting wildlife research (Sikes et al. 2016).

DATA AVAILABILITY STATEMENT

The data that support the findings of this study are available from the corresponding author upon request.

ORCID

Jessica Coltrane  <http://orcid.org/0009-0005-8902-6366>

REFERENCES

- Amburgey, S. M., A. A. Yackel Adams, B. Gardner, N. J. Hostetter, S. R. Siers, B. T. McClintock, and S. J. Converse. 2021. Evaluation of camera trap-based abundance estimators for unmarked populations. *Ecological Applications* 31:e02410.
- Ausband, D. E., P. M. Lukacs, M. Hurley, S. Roberts, K. Strickfaden, and A. K. Moeller. 2022. Estimating wolf abundance from cameras. *Ecosphere* 13:e3933.
- Buckland, S. T., J. M. Bretwick, K. L. Cattanach, and J. L. Laake. 1993. Estimated population size of the California gray whale. *Marine Mammal Science* 9:235–249.
- Burton, A. C., A. Neilson, D. Moreira, A. Ladle, R. Steenweg, J. T. Fisher, E. Bayne, and S. Boutin. 2015. Wildlife camera trapping: a review and recommendations for linking surveys to ecological processes. *Journal of Applied Ecology* 52:675–685.
- DeCesare, N. J., J. R. Newby, V. J. Boccadori, T. Chilton-Radandt, T. Their, D. Waltee, K. Podruzny, and J. A. Gude. 2016. Calibrating minimum counts and catch-per-unit-effort as indices of moose population trend. *Wildlife Society Bulletin* 40:537–547.
- DeCesare, N. J., and D. H. Pletscher. 2005. A dynamic test of spatial independence among bighorn sheep. *Intermountain Journal of Sciences* 11:25–30.
- DeCesare, N. J., and D. H. Pletscher. 2006. Movements, connectivity, and resource selection of Rocky Mountain bighorn sheep. *Journal of Mammalogy* 87:531–538.
- Forsyth, D. M., S. Comte, N. E. Davis, A. J. Bengsen, S. D. Côté, D. G. Hewitt, N. Morellet, and A. Mysterud. 2022. Methodology matters when estimating deer abundance: a global systematic review and recommendations for improvements. *Journal of Wildlife Management* 86:e22207.
- Gilbert, N. A., J. D. J. Clare, J. L. Stenglein, and B. Zuckerman. 2020. Abundance estimation of unmarked animals based on camera-trap data. *Conservation Biology* 35:88–100.
- Hofmeester, T. R., J. P. G. M. Cromsigt, J. Odden, H. Andrén, J. Kindberg, and J. D. C. Linnell. 2019. Framing pictures: a conceptual framework to identify and correct for biases in detection probability of camera traps enabling multi-species comparison. *Ecology and Evolution* 9:2320–2336.
- Hofmeester, T. R., J. M. Rowcliffe, and P. A. Jansen. 2017. A simple method for estimating the effective detection distance of camera traps. *Remote Sensing in Ecology and Conservation* 3:81–89.
- Howe, E. J., S. T. Buckland, M.-L. Després-Einspenner, and H. S. Kuhl. 2017. Distance sampling with camera traps. *Methods in Ecology and Evolution* 8:1558–1565.
- Leo, B. T. 2022. Evaluating unmarked abundance estimators using remote cameras and aerial surveys. *Wildlife Society Bulletin* 46:e1312.
- Loonam, K. E., P. M. Lukacs, D. E. Ausband, M. S. Mitchell, and H. S. Robinson. 2021. Assessing the robustness of time-to-event models for estimating wildlife abundance using remote cameras. *Ecological Applications* 31:e02388.
- Lula, E. S., B. Lowrey, K. M. Proffitt, A. R. Litt, J. A. Cunningham, C. J. Butler, and R. A. Garrott. 2020. Is habitat constraining bighorn sheep restoration? A case study. *Journal of Wildlife Management* 84:588–600.

- Lyet, A., S. Waller, T. Chambert, P. Acevedo, E. Howe, H. S. Kühl, R. Naidoo, T. O'Brien, P. Palencia, S. V. Soutyrina, et al. 2024. Estimating animal density using the space-to-event model and bootstrap resampling with motion-triggered camera-trap data. *Remote Sensing in Ecology and Conservation* 10:141–155.
- Moeller, A. K., and P. M. Lukacs. 2021. spaceNtime: an R package for estimating abundance of un marked animals using camera-trap photographs. *Mammalian Biology* 102:581–590.
- Moeller, A. K., P. M. Lukacs, and J. S. Horne. 2018. Three novel methods to estimate abundance of unmarked animals using remote cameras. *Ecosphere* 9:e02331.
- Moeller, A. K., S. J. Waller, N. J. DeCesare, M. C. Chitwood, and P. M. Lukacs. 2023. Best practices to account for capture probability and viewable area in camera-based abundance estimation. *Remote Sensing in Ecology and Conservation* 9:152–164.
- Montana Fish, Wildlife and Parks. 2010. Montana bighorn sheep conservation strategy. Montana Fish, Wildlife and Parks, Helena, USA.
- Nakashima, Y., K. Fukawawa, and H. Samejima. 2018. Estimating animal density without individual recognition using information derivable exclusively from camera traps. *Journal of Applied Ecology* 55:735–744.
- Pollock, K. H., J. D. Nichols, T. R. Simons, G. L. Farnsworth, L. L. Bailey, and J. R. Sauer. 2002. Large scale wildlife monitoring studies: statistical methods for design and analysis. *Environmetrics* 13:105–119.
- R Core Team. 2022. R: a language and environment for statistical computing. R Foundation for Statistical Computing, Vienna, Austria.
- Sikes, R. S., and Animal Care and Use Committee of the American Society of Mammalogists. 2016. 2016 Guidelines of the American Society of Mammalogists for the use of wild mammals in research and education. *Journal of Mammalogy* 97:663–688.
- Twining, J. P., C. McFarlane, D. O'Meara, C. O'Reilly, M. Reyne, W. I. Montgomery, S. Helyar, D. G. Tosh, and B. C. Augustine. 2022. A comparison of density estimation methods for monitoring marked and unmarked animal populations. *Ecosphere* 13:e4165.
- Zabransky, C. J., D. G. Hewitt, R. W. DeYoung, S. S. Gray, C. Richardson, A. R. Litt, and C. A. DeYoung. 2016. A detection probability model for aerial surveys of mule deer. *Journal of Wildlife Management* 80:1379–1389.

Associate Editor: Emily Sinnott.

How to cite this article: Coltrane, J., N. J. DeCesare, J. S. Horne, and P. M. Lukacs. 2024. Comparing camera-based ungulate density estimates: a case study using island populations of bighorn sheep and mule deer. *Journal of Wildlife Management* e22636. <https://doi.org/10.1002/jwmg.22636>